

Theoretical Study of the CH...X⁻ Interaction of Fluoromethanes and Chloromethanes with Fluoride, Chloride, and Hydroxide Anions

Eugene S. Kryachko[†] and Thérèse Zeegers-Huyskens*

Department of Chemistry, UniVersity of LeuVen, 200F Celestijnenlaan, B-3001 LeuVen, Belgium

Received: February 12, 2002; In Final Form: April 9, 2002

The present work focuses on the analysis of the CH...X⁻ interactions between Y_nH_{3-n}CH (n = 0-3, Y = F, Cl) as proton donors and X⁻ (X = F, Cl, OH) anions as proton acceptors using the MP2/6-31+G(d,p) method. The optimized geometries of these complexes and their vibrational frequencies and intensities are discussed. The changes in the populations of the relevant molecular orbitals are calculated using the natural bond orbital (NBO) analysis. The interaction energies range from 2.4 to 32.4 kcal mol⁻¹. The Y_nH_{3-n}CH (n = 0, 2, 3)X⁻ systems are stabilized by CH...X⁻ hydrogen bonds. It is demonstrated that the interaction results in an elongation of the incipient CH bond, a red shift of the ν(CH) vibration, and an increase of its intensity. The NBO analysis shows that the charge transfers go mainly to the σ*(CH) antibonding molecular orbital (MO) and, to a lesser extent, to the lone pairs of Y. It is also shown that the lengthening of the CH bond increases with the intermolecular distance and the increase of the population of the σ*(CH) MO. The interaction energies are correlated to the frequency shifts of the ν(CH) vibration. The CH₃YX⁻ complexes show contrasting behavior. The intermolecular distances and angles indicate that the CH₃Y molecules and the X⁻ anions are not stabilized by CH...X⁻ hydrogen bonds. In contrast with the other systems, complex formation causes a contraction of the CH bond, a blue shift of the ν(CH) vibration, a small decrease of the population of the σ*(CH) MO, and a marked increase of the population of the σ*(CY) MO. These features indicate that the CH₃YX⁻ systems are stabilized by electrostatic interactions and by charge transfer taking place in the remote part of the CH₃Y molecule.

1. Introduction

Since the early 1960s, crystallographic and spectroscopic studies have shown that CH groups can act as proton donors in hydrogen-bonded systems. In many cases, they control the molecular architecture to a large extent.¹ A variety of theoretical studies focusing on CH...O, CH...N, and CH...π interactions appeared recently. For many hydrogen bonds involving CH groups, an elongation of the CH bond and a red shift of the CH stretch have been detected in solution and in the gas phase as well.² There are a rather limited number of cases where, in contrast to conventional hydrogen bonds, the bridging CH bond is shortened and the corresponding stretching vibration is blue-shifted.³ A thorough analysis of the energies and populations of the molecular orbitals has led to the conclusion that there is actually no fundamental difference between the conventional OH...O and CH...O hydrogen bonds.^{3i,m}

For the conventional AH...B hydrogen bonds, correlations have been established between the interaction energy, the elongation of the AH bond, the frequency shift (or intensity) of the AH stretching vibration, and the intermolecular distance.⁴ On the contrary, as shown in our recent work,^{3m} for the complexes of fluoro- or chloromethanes with water, there is no correlation between the changes in the CH distance resulting from complex formation and the intermolecular distances or interaction energies. This intriguing behavior has been explained by the fact that in such CH...O systems the forces pushing toward contraction are slightly larger than the elongation forces,

whereas the opposite is valid for the conventional hydrogen bonds. It might be worth mentioning that in the aforementioned systems the interaction energies are low and vary over a small interval, between 0.3 and 3.8 kcal mol⁻¹, and the frequency shifts range from +9 to +43 cm⁻¹. In many aspects, the CHCl₃·H₂O complex appears to be a precursor of the conventional hydrogen bonds.

The main objective of the present work is to discuss the validity of the correlations existing for conventional hydrogen bonds for systems that involve CH proton donors. For this purpose, the interaction between methane, mono-, di-, and trisubstituted fluoro- and chloromethanes, on one hand, and F⁻, Cl⁻, and OH⁻ anions, on the other hand, is investigated. Such systems were chosen because the hydrogen bond energies are expected to be larger than those involving neutral bases as proton acceptors. Since the early 1980s, the interaction between CH groups and anions has been investigated by high-pressure mass spectrometry and ion cyclotron resonance spectroscopy.⁵ The experimental hydrogen-bond energies obtained for various CH proton donors and the F⁻ anion are large and fall between 25 and 30 kcal mol⁻¹.^{5d} Theoretical calculations are available for the structure and energy of the CH₄·Cl⁻ complex.⁶ This system has been investigated recently by pulsed electron beam spectroscopy.^{7a} Gas-phase equilibria for clustering reactions of the chloride ion with chloromethanes have also recently been measured by pulsed electron-beam high-pressure spectroscopy.^{7b} In this case, the interaction energies are also large, varying from 3.8 to 19.5 kcal mol⁻¹, on going from CH₄ to the more acidic proton donor CHCl₃. All of these studies deal with the structure and energies of the complexes, and except for the CH₄·Cl⁻

* Corresponding author. E-mail: therese.zeegers@chem.kuleuven.ac.be.

[†] On leave from Bogoliubov Institute for Theoretical Physics, Kiev, 03143 Ukraine.

complex, where a red shift of the CH stretching vibration has been theoretically predicted and experimentally observed,^{7a} vibrational data on other systems are unavailable. The same remark also holds for the charge distribution and the population of the molecular orbitals. As for the energies, we anticipate that these parameters vary within a broad interval. It is noteworthy that the interaction between methane derivatives, or more specifically, the methylhalides and the halide ions, may be important for bimolecular nucleophilic substitution (S_N2) reactions.⁸

This work is arranged as follows. In the first section, for the Y_nH_{3-n}CH (n = 0, 2, 3, Y = F, Cl) proton donors, we discuss the geometric changes resulting from interactions with the F⁻, Cl⁻ and OH⁻ anions. The second section deals with the interaction energies, vibrational frequencies, and infrared intensities of the ν(CH) stretching vibration. In the third section, we present the results of the natural bond orbital (NBO) analysis of the charge transfer and the change in occupation of the relevant molecular orbitals of the proton donor. In the last section, we discuss the same parameters for the interaction between the CH₃Y (Y = F, Cl) molecules and the F⁻ and Cl⁻ anions. For these systems, a totally different type of interaction is found, and these complexes, therefore, had to be treated separately.

2. Computational Methods

The geometries of the isolated molecules Y_nCH_{3-n} (n = 0-3, Y = F, Cl) and their complexes with the F⁻, Cl⁻, and OH⁻ anions were calculated at the MP2/6-31+G(d,p) level. These geometries were fully optimized without any constraints. The interaction energies were then determined as the difference in energy between the complex, on one hand, and the sum of the isolated monomers on the other hand. Basis set superposition errors (BSSE) were corrected by the counterpoise procedure.⁹ Harmonic vibrational frequencies and intensities of the isolated proton donor and the corresponding complexes with the anions were calculated at the same computational level. The charges on individual atoms, the population of the molecular orbitals, and the coefficients of the hybrid orbitals were obtained by using the natural bond population scheme.¹⁰ The Gaussian 98 package of programs¹¹ was used for all the calculations reported in the present work. All data refer to the standard conditions of 1 atm and 298 K.

3. Results and Discussion

Structure of the Complexes. Figure 1 schematically displays the structure of the complexes between Y_nH_{3-n}CH (n = 0, 2, 3, Y = F, Cl) and the F⁻, Cl⁻, and OH⁻ anions. The intermolecular distances, the CH...X⁻ angles, the changes of the length of the bridging CH bond and of the free CH' bond, along with the elongations of the CY bond resulting from the interaction with the anions, are gathered in Table 1.

In the case of the interaction between CH₄ and F⁻ or Cl⁻, the minimum-energy configuration is a C_{3v} structure in which F⁻ and Cl⁻ are bound to the vertex of the CH₄ tetrahedron. The hydrogen bond is almost linear. These data are in agreement with that of refs 7a and b. A face-bound C_{3v} structure, although being a stationary point as well, is placed 690 cm⁻¹ above the vertex-bound minimum.^{7a} In the CH₄...OH⁻ complex, the departure from linearity is slightly larger than that in the two other ones.

The complexes between CH₂Y₂ and the studied anions have an asymmetric bifurcated form. The CH...X⁻ angle ranges from

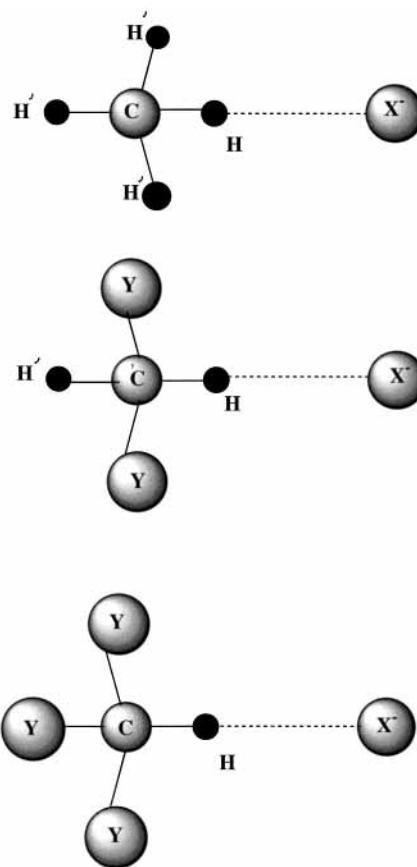


Figure 1. MP2/6-31+G(d,p) geometries of the CH₄...X⁻, CH₂Y₂...X⁻, and CHY₃...X⁻ complexes (Y = F, Cl; X = F, Cl, OH).

TABLE 1: MP2/6-31+G(d,p) Geometrical Parameters for the Interaction between Y_nH_{3-n}CH (n = 0, 2, 3) and F⁻, Cl⁻, and OH⁻

system	r(H...X ⁻), Å	∠CH...X ⁻ , deg	Δr(CH) ^a , mÅ	Δr(CH') ^a , mÅ	Δr(CY), mÅ
CH ₄ ...F ⁻	1.955	179.9	16.1	4.4	
CH ₄ ...Cl ⁻	2.730 ^b	178.2	2.7 ^b	2.4	
CH ₄ ...OH ⁻	2.040	173.4	12.9	4.5	
CH ₂ F ₂ ...F ⁻	1.699	164.1	21.7	2.4	26.8
CH ₂ F ₂ ...Cl ⁻	2.467	144.4	-1.7	0.4	16.1
CH ₂ F ₂ ...OH ⁻	1.802	151.4	12.0	1.4	26.2
CH ₂ Cl ₂ ...F ⁻	1.545	171.1	53.4	1.0	22.4
CH ₂ Cl ₂ ...Cl ⁻	2.288 ^c	162.4 ^c	9.4 ^c	-0.4	11.1
CH ₂ Cl ₂ ...OH ⁻	1.607	166.5	56.6	2.8	22.8
CHF ₃ ...F ⁻	1.537	179.7	51.3		26.0
CHF ₃ ...Cl ⁻	2.252	179.4	7.8		13.8
CHF ₃ ...OH ⁻	1.625 ^d	176.3	45.0		28.0
CHCl ₃ ...F ⁻	1.379	180.0	104.2		22.4
CHCl ₃ ...Cl ⁻	2.126	180.0	27.5		8.3
CHCl ₃ ...OH ⁻	1.431 ^d	177.0	101.0		19.1

^a Average of the values when the CH or CH' bonds are not entirely equivalent. ^b The calculated MP2(full)/aug-cc-pVTZ distance and elongation of the CH bond are 2.543 Å and 6 mÅ, respectively. ^{7a} ^c The H...X⁻ distance and the CH...X⁻ angle calculated at the QCISD(T)/6-311+G(d,p)//B3LYP/6-31+G(d) level are 2.30 Å and 156.9°, respectively. The elongation of the CH bond is 14 mÅ. ^{7b} ^d From ref 12.

144.4 to 171.1°, and the second hydrogen atom H' interacts with the anions weakly. If X⁻ = OH⁻, the H'...OH⁻ distances are relatively long: 3.129 Å for the CH₂F₂ complex and 3.184 Å for the CH₂Cl₂ complex. In both complexes, the atoms of the O...HCH' group lie in the same plane. In the CH₂Y₂...F⁻ complexes, the H...F⁻ distances are equal to 3.139 (Y = F) and 3.172 Å (Y = Cl).

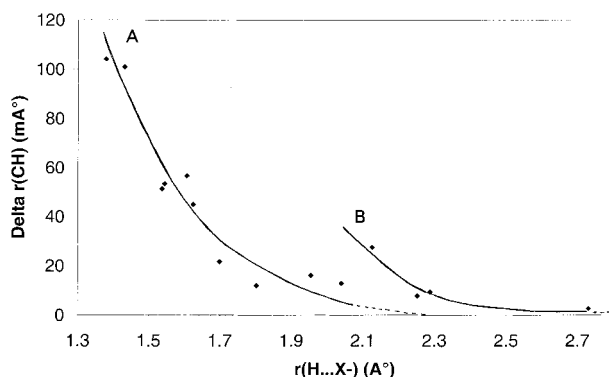


Figure 2. Elongations of the CH bond as a function of the intermolecular distances $r(\text{H}\cdots\text{X}^-)$ for $\text{Y}_n\text{H}_{3-n}\text{CH}$ ($n = 0, 2, 3$; $\text{Y} = \text{F}, \text{Cl}$) complexes. Curve A refers to the $\text{CH}\cdots\text{F}^-$ and $\text{CH}\cdots\text{OH}^-$ complexes, and curve B, to the $\text{CH}\cdots\text{Cl}^-$ complexes.

The $\text{CHY}_3\cdots\text{F}^-$ and $\text{CHY}_3\cdots\text{Cl}^-$ systems are characterized by C_{3v} symmetry. In the $\text{CHCl}_3\cdots\text{Cl}^-$ complex, the optimized $\text{H}\cdots\text{Cl}^-$ distance of 2.126 Å is somewhat smaller than the average $\text{H}\cdots\text{Cl}^-$ contact of 2.38 Å that is found in the crystalline state for CHCl_3 complexed with Cl^- anions.^{1g} In the $\text{CHY}_3\cdots\text{F}^-$ and $\text{CHY}_3\cdots\text{Cl}^-$ systems, the bridging proton resides preferentially closer to the C atom. In the $\text{CHCl}_3\cdots\text{F}^-$ complex characterized by a perfectly collinear hydrogen bond, the $\text{C}\cdots\text{F}^-$ distance is very short, 2.567 Å, although it is still about 0.3 Å longer than it is in the $(\text{FHF})^-$ ion.¹² The corresponding hydrogen bond is not symmetrical, the CH distance of 1.188 Å being smaller than the intermolecular $\text{H}\cdots\text{F}^-$ distance of 1.379 Å. For this complex, the elongation of the CH bond is very large, 104.2 mÅ. The complexes between CHY_3 and OH^- are stationary points on the potential energy surface. However, as shown in a recent work,¹³ the most stable structures are the proton-transferred ones, $\text{Y}_3\text{C}^-\cdots\text{H}_2\text{O}$, which are energetically favored by 1.1 kcal mol⁻¹ (F_3CH) and 7.1 kcal mol⁻¹ (Cl_3CH) over the $\text{Y}_3\text{CH}\cdots\text{OH}^-$ structures. From these data, we have concluded that proton transfer occurs if the difference between the proton affinity (PA) of the X^- anion and the proton affinity of the CY_3^- anion is at least 8 kcal mol⁻¹.

As follows from Table 1, the intermolecular distances, ranging from 1.379 to 2.730 Å, are smaller than the sum of the van der Waals radii of the hydrogen atom and the anions, and the $\text{CH}\cdots\text{X}^-$ angles significantly exceed 90°. It therefore seems, following the criteria of ref 1c, that all of the CH proton donors and the anions listed in Table 1 are held together by $\text{CH}\cdots\text{X}^-$ hydrogen bonds. Furthermore, the interaction operates to elongate the CH bond by 2.7 to 104.2 mÅ, except in the $\text{CH}_2\text{F}_2\cdots\text{Cl}^-$ complex, whose CH bond is slightly contracted. It is worth noticing, particularly for the following discussion, that the latter complex is characterized by the largest departure from linearity of the $\text{CH}\cdots\text{X}^-$ bond. The CH' bond is also lengthened, although to a much smaller extent than the CH bond. As indicated by the data of Table 1, the elongations of the CH and CH' bonds are not correlated to each other.

For the $\text{CH}\cdots\text{O}$ hydrogen bonds, the lengthening of the CH bond (~ 10 mÅ) is just discernible by diffraction methods, so no correlation could be found between the experimental CH and $\text{H}\cdots\text{O}$ distances.^{1f} However, for the $\text{CH}\cdots\text{X}^-$ hydrogen bonds, the elongation of the CH bond is much larger, and the intermolecular distances vary within a much broader interval. It is therefore possible to find a correlation between these two parameters. Such a correlation is illustrated in Figure 2. We notice that very similar correlations were obtained for hydrogen bonds involving NH groups. The $\text{NH}\cdots\text{O}$ and $\text{NH}\cdots\text{F}$ systems

TABLE 2: MP2/6-31+G(d,p) Interaction Energies Calculated without and with Counterpoise Correction of BSSE, Frequency Shifts of the $\nu(\text{CH})$ Vibration, and Square Root of the Intensity Increase of the $\nu(\text{CH})$ Vibration in the Complexes between $\text{Y}_n\text{H}_{3-n}\text{CH}$ ($n = 0, 2, 3$, $\text{Y} = \text{F}, \text{Cl}$) and F^- , Cl^- , and OH^-

system	$E(\text{without BSSE})$, kcal mol ⁻¹	$E(\text{with BSSE})$, kcal mol ⁻¹	$\Delta\nu(\text{CH})$ cm ⁻¹	$\times \Delta I$, km ^{1/2} mol ^{-1/2}
$\text{CH}_4\cdots\text{F}^-$	5.57	4.78	- 234	17.8
$\text{CH}_4\cdots\text{Cl}^-$	2.45 ^a	1.58	- 32 ^b	6.6
$\text{CH}_2\cdots\text{OH}^-$	5.90	4.55	- 179	16.5
$\text{CH}_2\text{F}_2\cdots\text{F}^-$	20.22	20.41	- 321	20.4
$\text{CH}_2\text{F}_2\cdots\text{Cl}^-$	12.54	11.52	+ 27	
$\text{CH}_2\text{F}_2\cdots\text{OH}^-$	21.03	20.36	- 207	16.5
$\text{CH}_2\text{Cl}_2\cdots\text{F}^-$	23.59 ^c	23.16	- 777	34.9
$\text{CH}_2\text{Cl}_2\cdots\text{Cl}^-$	13.82	11.74	- 137	21.0
$\text{CH}_2\text{Cl}_2\cdots\text{OH}^-$	24.34	22.75	- 733	32.3
$\text{CHF}_3\cdots\text{F}^-$	27.65	29.26	- 719	29.8
$\text{CHF}_3\cdots\text{Cl}^-$	16.62	15.11	- 124	15.1
$\text{CHF}_3\cdots\text{OH}^-$	27.59	27.82	- 678	30.0
$\text{CHCl}_3\cdots\text{F}^-$	31.04	32.68	- 1422	51.2
$\text{CHCl}_3\cdots\text{Cl}^-$	18.24 ^d	15.0	- 318	32.1
$\text{CHCl}_3\cdots\text{OH}^-$	32.42	33.07	- 1511	54.3

^a Experimental value) 3.8 kcal mol⁻¹.^{7b} ^b The calculated MP2(full)/aug-cc-pVTZ shifts for the hydrogenated isotopomer are - 34 and - 60 cm⁻¹ for the split components of the F vibration and - 55 cm⁻¹ for the A_1 vibration.^{7a} ^c Experimental value) 14.8 kcal mol⁻¹.^{7b} ^d Experimental value) 19.5 kcal mol⁻¹.^{7b}

are situated on the same curve, and the $\text{NH}\cdots\text{Cl}$ system is strongly shifted to the right,^{1a} which is obviously due to the larger van der Waals radius of the Cl atom (1.80 Å) compared with that of the H and F atoms (1.2 and 1.35 Å, respectively).

Interaction Energies, Frequency Shifts, and Intensities of the $\nu(\text{CH})$ Vibration. Table 2 reports the interaction energies (E) calculated without and with BSSE corrections. There appears to be some inconsistency related to the BSSE-corrected values; therefore, they seem to be less reliable than the noncorrected ones. Indeed, chloroalkanes can be considered to be better proton donors than fluoroalkanes.¹⁴ However, the BSSE-corrected values of the interaction energies for the Cl^- complexes are nearly the same for the chloro- and fluoroalkanes. Furthermore, the OH^- anion is a stronger proton acceptor than is the F^- anion, although for CH_2Y_2 complexed with these two anions nearly the same interaction energies are obtained. Interestingly, these discrepancies disappear when dealing with the BSSE uncorrected energies, which will be further considered in the present work. It is also worth noticing that the experimental energies obtained for the standard state of 1 atm^{7b} are closer to the uncorrected values than to the corrected ones (Table 2). It is likely that such an inconsistency between BSSE-corrected and uncorrected interaction energies is due to the rather small basis set employed in the present work that poorly describes the polarization and dispersion terms of the interaction energies of the studied systems.

The frequency shifts ($\Delta\nu$) and the square root of the intensity enhancement ($\times \Delta I$) of the $\nu(\text{CH})$ vibration caused by complex formation are also collected in Table 2. To obtain reliable spectroscopic data, we have calculated the frequencies and intensities for the $\text{CHD}'\text{Y}_2$ and $\text{CD}'_3\text{H}$ isotopes where the CH bond acts as a proton donor and the CD' bonds do not directly interact with the anion. Mixing the free and complexed $\nu(\text{CH})$ vibrations can indeed substantially influence their frequencies and intensities. In isolated CH_4 , for example, the triply degenerate vibration F is predicted to occur at 3265 cm⁻¹ and the A_1 vibration, at 3120 cm⁻¹. In the $\text{CH}_4\cdots\text{F}^-$ complex, the doubly degenerate vibration E, calculated to occur at 3146 cm⁻¹, involves mainly a displacement of the free CH' bond, but the two components at 3146 and 2953 cm⁻¹, which are red-shifted

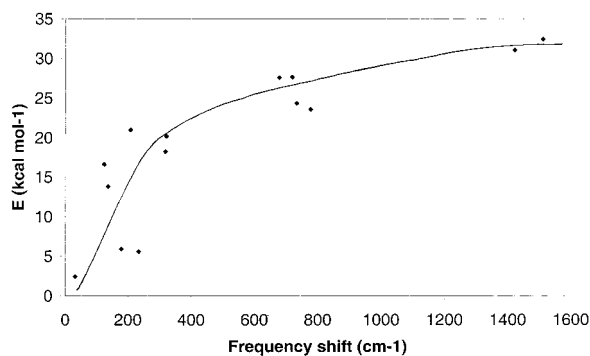


Figure 3. Interaction energies as a function of the frequency shifts of the $\nu(\text{CH})$ vibration.

by 119 and 312 cm^{-1} from the vibrational frequencies of the free molecule, include vibrations of both the CH and CH' bonds. The vibration predicted at 3234 cm^{-1} in free CD_3H describes only a displacement of the CH bond. This mode is shifted to 3000 cm^{-1} in the CH_4F^- complex. Thus, the value of -234 cm^{-1} represents the real shift resulting from complex formation. Similar comments also hold for the intensity changes of the $\nu(\text{CH})$ vibration. The infrared intensity, which is equal to 17 km mol^{-1} in the free CD_3CH isotopomer, increases to 335 km mol^{-1} in its complex with F^- .¹⁵ We must also mention that in the $\text{CHD}'\text{Cl}_2\text{F}^-$ complex two vibrational modes that are shifted by -751 and -804 cm^{-1} with respect to the free molecule both include large contributions from the $\nu(\text{CH})$ and $\nu(\text{CD}')$ modes. In this case, the average value of the two frequency shifts is considered.

The data reported in Table 2 indicate that the interaction energies vary over a very broad range, from 2.4 to $32.4\text{ kcal mol}^{-1}$. It is also worth mentioning that the interaction energy between CHCl_3 and F^- is large: 31 kcal mol^{-1} . However, this value is smaller than that for the symmetrical $(\text{FHF})^-$ ion: 40 – 44 kcal mol^{-1} .¹² We also notice large perturbations of the $\nu(\text{CH})$ vibrations, which are all red-shifted by -32 to -1511 cm^{-1} , except in the $\text{CH}_2\text{F}_2\text{Cl}^-$ system, where a blue shift resulting from a contraction of the CH bond is predicted. The present data demonstrate, for all other systems, the existence of a rough correlation between the calculated interaction energies and the harmonic frequency shifts of the relevant CH stretching vibrations, the so-called Badger- Bauer relation.¹⁶ Such correlation, illustrated in Figure 3, shows great departure from linearity. A similar effect was also observed for $\text{OH}\cdots\text{O}$ systems when considering a broad energy range.¹⁷ As discussed by Sandorfy,^{18a} it might appear astonishing that good relationships have been obtained between the hydrogen bond energies and the experimental (anharmonic) frequency shifts. The explanation is that, as demonstrated for different hydrogen-bonded systems,^{18b-d} the changes in anharmonicity are roughly proportional to the interaction energies. Thus, the Badger- Bauer correlation holds for harmonic and anharmonic frequency shifts as well but is characterized by different slopes and intercepts.^{18b} This is likely to be the case for the present complexes. It is also worth mentioning that for transitions involving a single minimum the vibrations become superharmonic, and the anharmonicity correction has been estimated to increase the calculated harmonic frequency.^{18e,f} However, as discussed in the first section, all of the complexes investigated in the present work, even the strongest one, CHCl_3F^- , have a double minimum potential.

The results of Table 2 also demonstrate that the square root of the intensity enhancement of the $\nu(\text{CH})$ vibration increases with increasing frequency shift.

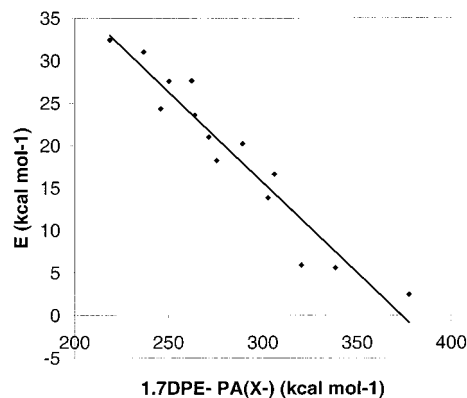


Figure 4. Interaction energies as a function of $1.7\text{ DPE} - \text{PA}(\text{X}^-)$.

It has been recently shown¹⁹ that the hydrogen bond strength qualitatively parallels an increase of the acidity of the CH proton donor. For hydrogen bonds involving various CH proton donors and a constant proton acceptor like a water molecule, correlations exist between the hydrogen bond strength and the deprotonation energy (DPE) of the proton donor.^{31,3m} For the present complexes, the interaction energies relative to a given anion are, as expected, linearly correlated to the DPE of the CH proton donors. The correlation coefficients vary from 0.967 to 0.985 . The slopes and intercepts depend on the nature of the anion. For complexes involving different proton acceptors and donors, the interaction energies can be expressed as a function of the differences in DPE and PA of the isolated molecules or anions. For the present complexes, a plot of E versus $(\text{DPE} - \text{PA})$ gives a correlation coefficient of only 0.863 . The best correlation coefficient is found for the following equation:

$$E) 0.212 + (1.7\text{ DPE} - \text{PA}(\text{X}^-)) \quad r) 0.9604$$

This relation illustrated in Figure 4 clearly demonstrates that the acidity plays a more important role in determining the hydrogen bond energies than does the basicity of the proton acceptor. The correlations, deduced for the interaction between neutral molecules and more specifically, the interaction between nucleobases and water,²⁰ can now be extended to $\text{CH}\cdots\text{X}^-$ hydrogen bonds.

NBO Analysis of the Electronic Structure. The formation of a hydrogen bond complex implies that a certain amount of electronic charge is transferred from the proton acceptor to the proton donor molecule. In addition, a rearrangement of electronic density within each monomer occurs. In conventional hydrogen bonds such as $\text{OH}\cdots\text{O}$ or $\text{OH}\cdots\text{N}$, the decrease of the AH stretching frequencies is consistent with the bond weakening associated with increasing occupation of the $\sigma^*(\text{AH})$ antibonding molecular orbital (MO). Table 3 lists the charge transfer (CT), the change in occupation of the $\sigma^*(\text{CH})$ antibonding MO and of the lone pairs of each Y atom of the studied complexes $\text{Y}_n\text{H}_{3-n}\text{CH}\text{X}^-$ ($n = 1$). These results show that the charge that is transferred from the anion to the proton donor goes mainly into the $\sigma^*(\text{CH})$ MO and to the lone pair of the Y atom. Furthermore, as illustrated in Figure 5, there is an almost linear correlation between the elongation of the CH bond and the change in the population of the corresponding $\sigma^*(\text{CH})$ antibonding MO.

The present results further indicate that the amount of charge transfer does not exactly match the sum of the changes in the population of the $\sigma^*(\text{CH})$ orbitals and of the lone pairs of Y. The differences can be accounted for by small variations in the populations of the other orbitals of the proton donor. In the three

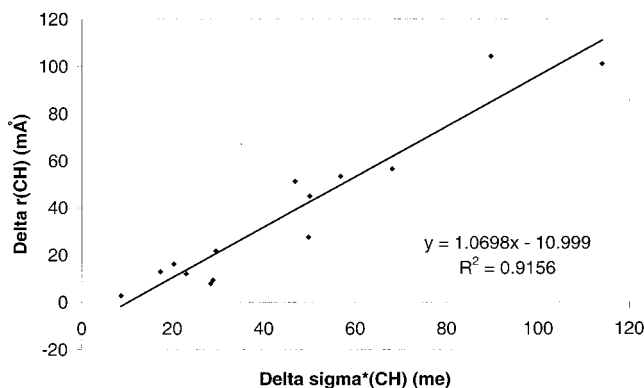


Figure 5. Elongation of the CH bond as a function of the increase of the population of the $\sigma^*(\text{CH})$ antibonding MO.

TABLE 3: Charge Transfer and Changes in the Occupation of the $\sigma^*(\text{CH})$ Orbital and of the Lone Pairs of Y (me) in the Complexes between $\text{Y}_n\text{H}_{3-n}\text{CH}$ ($n = 0, 2, 3$, Y = F, Cl) and F^- , Cl^- and OH^-

system	CT	$\Delta\sigma^*(\text{CH})$	ΔLP
$\text{CH}_4\hat{\text{a}}\text{F}^-$	21.7	20.3	
$\text{CH}_4\hat{\text{a}}\text{Cl}^-$	8.9	8.7	
$\text{CH}_4\hat{\text{a}}\text{OH}^-$	17.5	17.4	
$\text{CH}_2\text{F}_2\hat{\text{a}}\text{F}^-$	44.0	29.5	10.9
$\text{CH}_2\text{F}_2\hat{\text{a}}\text{Cl}^-$	20.4	10.9	7.6
$\text{CH}_2\text{F}_2\hat{\text{a}}\text{OH}^-$	35.0	23.0	11.2
$\text{CH}_2\text{Cl}_2\hat{\text{a}}\text{F}^-$	73.9	56.8	11.4
$\text{CH}_2\text{Cl}_2\hat{\text{a}}\text{Cl}^-$	40.5	28.9	7.8
$\text{CH}_2\text{Cl}_2\hat{\text{a}}\text{OH}^-$	84.8	68.1	11.6
$\text{CHF}_3\hat{\text{a}}\text{F}^-$	72.0	46.9	13.8
$\text{CHF}_3\hat{\text{a}}\text{Cl}^-$	45.2	28.4	9.3
$\text{CHF}_3\hat{\text{a}}\text{OH}^-$	75.0	50.0	13.0
$\text{CHCl}_3\hat{\text{a}}\text{F}^-$	117.9	89.7	12.5
$\text{CHCl}_3\hat{\text{a}}\text{Cl}^-$	69.9	49.8	8.4
$\text{CHCl}_3\hat{\text{a}}\text{OH}^-$	145.0	114.0	12.7

$\text{CH}_4\hat{\text{a}}\text{Cl}^-$ complexes, we observe a small increase of the population of the $\sigma^*(\text{CH})$ orbital and of the Rydberg orbitals of the carbon atom as well. In contrast, we notice a small decrease of the populations of the $\sigma^*(\text{CH})$ and $\sigma^*(\text{CY})$ MOs and of the Rydberg orbitals of the carbon atom for all other complexes. In the $\text{CHCl}_3\hat{\text{a}}\text{Cl}^-$ complex, for example, the decrease of the $\sigma^*(\text{CY})$ population is equal to 1.4 me, and the decrease of the population of the Rydberg orbital of the C atom takes the value of 4.5 me.

Charge density on the individual C and H atoms must be considered with caution. Indeed, whereas the hydrogen atom acquires a positive charge in all the monomers, the natural charges on the C atom depend on the nature of the halogenomethanes and cover a wide range of values and reversed signs. However, a common feature of all the studied complexes is the increase of the charge on the C atom and a decrease of the charge on the H atom, leading to enhanced $\text{C}^- - \text{H}^+$ polarization. For example, in the strong $\text{CHCl}_3\hat{\text{a}}\text{F}^-$ complex, the C atom gains 0.03 e and the H atom loses 0.18 e.

Complex formation also results in an increase of the percentage of s character of the CH bond from 25 to 29% in the weakest $\text{CH}_4\hat{\text{a}}\text{Cl}^-$ complex and from 32 to 40% in the strongest $\text{CHCl}_3\hat{\text{a}}\text{F}^-$ and $\text{CHCl}_3\hat{\text{a}}\text{OH}^-$ complexes.

To visualize the formation of the $\text{CH}\hat{\text{a}}\text{aX}^-$ bond in terms of the MO pattern, we present in Figure 6 the electron density difference section of the $\text{CHF}_3\hat{\text{a}}\text{F}^-$ complex.²¹ It clearly shows the charge transfer from H, which loses electron density to F^- under the formation of the $\text{CH}\hat{\text{a}}\text{aF}^-$ hydrogen bond. A substantial gain of density occurs on the fluorine of CHF_3 .

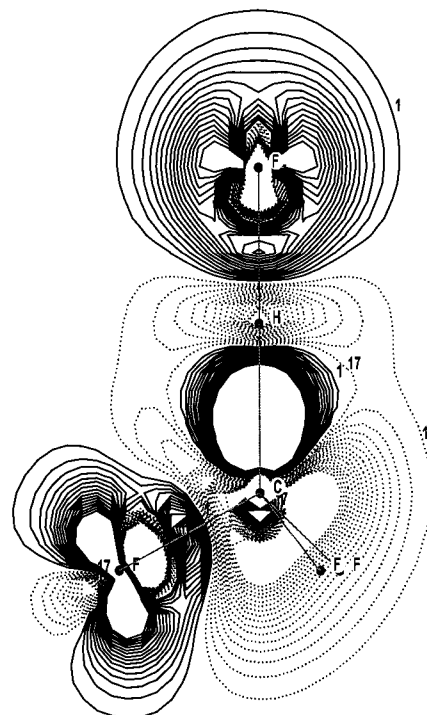


Figure 6. Electron density difference distribution of the $\text{CHF}_3\hat{\text{a}}\text{F}^-$ complex using the MOLDEN program.²⁰ The contour spacing is 0.00250 e/au^3 . Contour 1 refers to the value of 0.00250 e/au^3 whereas contour 17 refers to the value of -0.00250 e/au^3 . Dotted lines represent a loss of electron density relative to that of isolated CHF_3 and F^- . Dark regions correspond to an increase in the density.

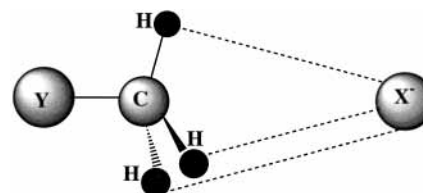


Figure 7. MP2/6-31+G(d,p) geometry of the $\text{CH}_3\text{Y}\hat{\text{a}}\text{X}^-$ complexes (Y = F, Cl; X = F, Cl).

Interaction between CH_3Y (Y = F, Cl) and the F^- and Cl^- Anions. In this section, we comment on the interaction between CH_3Y (Y = F, Cl) and the F^- and Cl^- anions. The structure of such complexes is schematically displayed in Figure 7, which shows that the X^- anion is coordinated to the C_{3v} principal axis of the methylhalide. We notice that an analogous structure has recently been found for the $\text{CH}_3\text{Cl}\hat{\text{a}}\text{Cl}^-$ complex using the B3LYP/6-31+G(d) method: $r(\text{H}\hat{\text{a}}\hat{\text{a}}\hat{\text{a}}\text{Cl}^-)$ 3.06 Å and the $\text{CH}\hat{\text{a}}\hat{\text{a}}\hat{\text{a}}\text{Cl}^-$ angle has not been mentioned.^{7b} The present geometric parameters including the intermolecular $\text{H}\hat{\text{a}}\hat{\text{a}}\hat{\text{a}}\text{X}^-$ distances and $\text{CH}\hat{\text{a}}\hat{\text{a}}\hat{\text{a}}\text{X}^-$ angles along with the variations of the CY and CH distances are listed in Table 4. The intermolecular distances range from 2.472 to 3.082 Å. Surprisingly, they are not ordered according to the proton donor ability of the methylhalide. Indeed, these distances are longer than those for the complexes involving the weaker proton donor CH_4 . Furthermore, the $\text{H}\hat{\text{a}}\hat{\text{a}}\hat{\text{a}}\text{Cl}^-$ distance is almost the same in the $\text{CH}_3\text{F}\hat{\text{a}}\text{Cl}^-$ and $\text{CH}_3\text{Cl}\hat{\text{a}}\text{Cl}^-$ complexes, despite the larger acidity of CH_3Cl .¹⁴ We also notice that the intermolecular distances are slightly shorter than the sum of the van der Waals distances (2.55 Å) for the F^- complexes and slightly longer than this sum (3.0 Å) for the Cl^- complexes. The $\text{CH}\hat{\text{a}}\hat{\text{a}}\hat{\text{a}}\text{X}^-$ angles vary between 84.1 and 89.5°. Noting that hydrogen bond character decreases with the decreasing donor-acceptor angle and es-

TABLE 4: MP2/6-31+G(d,p) Geometrical Parameters, Variations of the CH and CY Bond Distances, and Frequency Shifts of the $\nu(\text{CH})$ Vibration for the Interaction between CH₃Y (Y = F, Cl) and F⁻ and Cl⁻

system	$r(\text{H}\cdots\text{X}^-)$ Å	$\angle\text{CH}\cdots\text{X}^-$, deg	$\Delta r(\text{CY})$, mÅ	$\Delta r(\text{CH})$, Å	$\Delta\nu(\text{CH})^a$, cm ⁻¹
CH ₃ F \cdots F ⁻	2.501	83.5	48.7	- 6.5	81
CH ₃ F \cdots Cl ⁻	3.082	88.6	31.1	- 4.3	56
CH ₃ Cl \cdots F ⁻	2.472	84.1	52.9	- 6.2	39
CH ₃ Cl \cdots Cl ⁻	3.081	89.5	30.1	- 3.9	54

^a Frequency shift of the E vibration of the CH₃ group.

TABLE 5: Interaction Energies, Charge Transfers, and Changes in the Occupation of the $\sigma^*(\text{CH})$ and $\sigma^*(\text{CY})$ MO and of the Lone Pairs of Y for the Interaction between CH₃Y (Y = F, Cl) and F⁻ and Cl⁻

system	E^a	CT	$\Delta\sigma^*(\text{CH})$	$\Delta\sigma^*(\text{CY})$	ΔLP
CH ₃ F \cdots F ⁻	13.91(13.51)	16.3	- 1.9	17.8	9.0
CH ₃ F \cdots Cl ⁻	6.04(5.34)	10.7	- 1.4	10.9	6.5
CH ₃ Cl \cdots F ⁻	13.98(13.24)	18.7	- 1.8	19.2	9.6
CH ₃ Cl \cdots Cl ⁻	9.55(8.55)	11.4	- 1.2	10.8	6.7

^a The values in parentheses are the BSSE-corrected values.

sentially vanishes around 90°,^{1c,f} we conclude that these highly bent geometries do not actually correspond to a hydrogen bonding interaction. These features clearly indicate that the interaction is electrostatic, in agreement with the statement of ref 7b. It is also worth mentioning that, as shown in ref 7b, the ion-dipole complex geometry in (CH₃Cl)_nCl⁻ can be extended to those of large clusters. The fact that the H \cdots Cl⁻ distance of 3.06 Å for $n = 1$ is almost the same as that for $n = 2$ indicates the electrostatic nature of the interaction. However, for a hydrogen bond, anticooperativity should lead to an increase of the H \cdots Cl⁻ distance with increasing n .²²

For all of the CH₃Y \cdots X⁻ systems, complex formation results in a weak contraction of the CH bond from 3.9 to 6.5 mÅ. This contraction parallels a blue shift of 39–81 cm⁻¹ of the corresponding $\nu(\text{CH})$ vibration and a decrease of its infrared intensity by a factor of 0.4–0.6. We also note that, in contrast with the complexes involving the other halomethanes, a relatively large lengthening of the CY bonds takes place.

The interaction energies and the results of the NBO analysis (CT and population changes) are given in Table 5. The interaction energies vary from 6 to 13.9 kcal mol⁻¹. It is worth mentioning that they are not ordered according to the acidity of the proton donor. The acidity of CH₃Cl is larger than the acidity of CH₃F¹⁴ by 13 kcal mol⁻¹, but the same energy of 13.9 kcal mol⁻¹ is calculated for the interaction with F⁻.

Despite the nonlinearity of the intermolecular CH \cdots X⁻ bonds, the CT occurring from the X⁻ anion to the CH₃Y molecule takes relatively large values, varying from 10.7 to 18.7 me. Interestingly, these values are of the same order of magnitude as those obtained for the CH₄ complexes, being somewhat weaker for the F⁻ complexes, on one hand, and somewhat larger for the Cl⁻ complexes, on the other hand. This implies that the CT, like the intermolecular distances or interaction energies, does not actually follow the order predicted by the acidity of the proton donor. Furthermore, the charge transferred from the anion to the neutral molecule mainly goes to the $\sigma^*(\text{CY})$ antibonding MO and to a lesser extent to the lone pairs of Y. The population of the $\sigma^*(\text{CH})$ MO slightly decreases by 1.2 to 1.9 me. As mentioned above, such a decrease parallels a small contraction of the CH bond and a blue shift of the $\nu(\text{CH})$ vibration.

The last difference concerns the charges on the C and H atoms. In the CH₃Y \cdots X⁻ complexes, the carbon atom loses

electronic density whereas the H atom becomes slightly more positive, which indicates decreasing polarity of the CH bond. For example, in the CH₃Cl \cdots F⁻ complex, the C atom loses 0.08 e and the H atom, about 0.02 e. Thus, the results of the NBO analysis also clearly indicate that the nature of the interaction in the CH₃Y \cdots X⁻ complexes is different from that in the CH₄ \cdots X⁻, CH₂Y₂ \cdots X⁻, and CHY₃ \cdots X⁻ complexes. The present data suggest that the present systems are largely stabilized by electrostatic interaction and by CT taking place in the remote part of the CH₃Y molecule.

As mentioned above, in the complex CH₂F₂ \cdots Cl⁻, the CH \cdots X⁻ angle is smaller than those in the other CH₂Y₂ \cdots X⁻ or CHY₃ \cdots X⁻ systems, which means that the CH₂F₂ \cdots Cl⁻ complex is stabilized not only by the CH \cdots Cl⁻ hydrogen bond but also by a secondary interaction between the CH' bond and Cl⁻. This is, in some sense, an intermediate complex, where the interaction results in a weak contraction of the CH bond, a blue shift of the $\nu(\text{CH})$ vibration, and an increase of the population of the $\sigma^*(\text{CH})$ orbital.

Finally, we would like to address some comments on recent MP2/6-311G(d,p) calculations on the CH₃Br \cdots Cl⁻ complex.^{6b} The H \cdots Cl⁻ distance and the CH \cdots Cl⁻ angle have not been indicated in ref 6b. However, the fact that the intermolecular distances calculated in the present work are almost the same as those for the CH₃F \cdots Cl⁻ and CH₃Cl \cdots Cl⁻ complexes suggests that these distances are likely to be the same in the CH₃Br \cdots Cl⁻ complex. Furthermore, the latter complex possesses other features that are very similar to the CH₃Cl \cdots Cl⁻ complex: $\Delta r(\text{CH}) = -4$ mÅ, $\Delta r(\text{CY}) = 35.4$ mÅ, $\Delta\nu^{\text{as}}(\text{CH}) = 44$ cm⁻¹, and $\Delta\nu^{\text{s}}(\text{CH}) = 57$ cm⁻¹.^{6b} Altogether, this data strongly suggests that the CH₃Br molecule and the Cl⁻ anion are held together by electrostatic interactions rather than by three bifurcated CH \cdots X⁻ hydrogen bonds, as claimed in ref 6b. This statement also agrees with the similar permanent dipole moments of CH₃F (1.86 D), CH₃Cl (1.89 D), and CH₃Br (1.82 D).

General Conclusions. The present work focuses on a theoretical study of the interaction between Y_nH_{3-n}CH (n = 0–3, Y = F, Cl) and X⁻ anions (X = F, Cl and OH). These systems have been chosen because their interaction energies, spectroscopic parameters, and populations of the relevant MO orbitals were expected to vary within a broad range. The main objective of this work is to analyze whether the relations among the interaction energies, the elongation of the CH bond, the intermolecular distances, and the infrared frequency shifts, established for conventional hydrogen bonds, are valid for ionic CH \cdots X⁻ hydrogen bonds. In the studied systems involving the Y_nH_{3-n}CH (n = 0, 2, 3) molecules and the X⁻ anions, the interaction energies vary from 2.4 to 32.4 kcal mol⁻¹. We have shown that they correlate fairly well with the intermolecular distances, similarly to that of hydrogen bonds involving NH groups. As also demonstrated, the interaction energies correlate to the deprotonation enthalpies of the CH bond of the proton donors and to the proton affinity of the anions. Hydrogen bond formation results in a lengthening of the recipient CH bond, a red shift of the $\nu(\text{CH})$ vibration, and an enhancement of its infrared intensity. The Badger–Bauer correlation between the interaction energies and the frequency shifts of the $\nu(\text{CH})$ vibration appears to be valid for the studied systems, although it shows a large departure from linearity. The NBO analysis demonstrates that the charge transfer from the anion to the proton acceptor goes mainly to the $\sigma^*(\text{CH})$ antibonding MO and, to a lesser extent, to the lone pair of the Y atom. As for conventional hydrogen bonds, the lengthening of the CH bond increases with increasing population of the $\sigma^*(\text{CH})$ MO. The

systems involving the CH₃Y (Y = F, Cl) molecules and the F⁻ and Cl⁻ anions show a totally different type of interaction. The values of the intermolecular distances and angles suggest that the molecules and ions are not held together by hydrogen bonds. Their complex formation results in a contraction of the recipient CH bond, a blue shift of the ν(CH) vibration, and a decrease of its infrared intensity. Furthermore, the NBO analysis indicates that complexation causes a small decrease of the population of the σ*(CH) MO. The charge transfer goes mainly to the σ*(CY) MO and, to a lesser extent, to the lone pairs of the Y atom.

Finally, we would like to address some comments on the so-called H index, which is defined as the ratio of charge transferred to the σ*(CH) MO to the total charge transfer between the proton acceptor and donor.²³ The value of this index should be 0.7–1 for hydrogen-bonded complexes and should approach unity for very strong hydrogen bonds whereas values between 0.3 and 0 should be typical for improper blue-shifting hydrogen bonds. For the complexes investigated in the present work, the H index takes the following values: for the CH₄·X⁻ complexes, it varies from 0.93 to 0.98; for the CH₂Y₂·X⁻ complexes, from 0.53 to 0.80; and for the CHY₃·X⁻ complexes, from 0.63 to 0.79. Overall, these results clearly demonstrate that, contrary to the statements of ref 22, the H index is larger for the weaker CH₄·X⁻ complexes and does not show any regularity for the other complexes. We have recently studied the CH₄·O interaction in fluoromethane·H₂O and chloromethane·H₂O complexes.^{3m} Our results indicate that for these systems the H index varies from 1 for the weakest CH₄·H₂O complex to 0.48 for the strongest CHCl₃·H₂O complex. These results can be accounted for by the fact that the overall charge transfer, taking place from the O lone pairs to the proton donor, increases with the number of halogen atoms implanted on the C atom. Furthermore, the H index is unlikely to be negative. Indeed, in all of the CH hydrogen bonds investigated to date, including the blue-shifting ones, there is always an increase of the σ*(CH) population.^{3m,10,13}

Acknowledgment. E.S.K. acknowledges a grant of the University of Leuven.

References and Notes

- (1) For leading references, see (a) Pimentel, C. G.; McClellan, A. L. *The Hydrogen Bond*; W. H. Freeman and Co.: San Francisco, 1960. (b) Green, R. D. *Hydrogen Bonding by CH Groups*; Macmillan: London, 1974. (c) Taylor, R.; Kennard, O. *J. Am. Chem. Soc.* **1982**, *104*, 5063. (d) Jeffrey, G. A. *An Introduction to Hydrogen Bonding*; Oxford University Press: New York, 1997. (e) Scheiner, S. *Hydrogen Bonding: A Theoretical Perspective*; Oxford University Press: New York, 1997. (f) Desiraju, G. R.; Steiner, T. *The Weak Hydrogen Bond in Structural Chemistry and Biology*; Oxford University Press: New York, 1999. (g) Steiner, T. *New J. Chem.* **1998**, *1099*. (h) Vargas, R.; Garza, J.; Friesner, R. A.; Stern, R. A.; Hay, B. P.; Dixon, D. A. *J. Phys. Chem. A* **2001**, *105*, 4963. (i) Raymo, F. M.; Bartberger, M. D.; Houk, K. N.; Stoddart, J. F. *J. Am. Chem. Soc.* **2001**, *123*, 9264 and references therein.
- (2) (a) Allerhand, A.; Schleyer, P. v. R. *J. Am. Chem. Soc.* **1963**, *85*, 1715. (b) Hussein, M. A.; Millen, D. *J. Chem. Soc., Faraday Trans. 2* **1976**, *72*, 693. (c) Devaure, J.; Turrell, G.; Van Huong, P.; Lascombe, J. *J. Chim. Phys.* **1968**, *65*, 1064. (d) Rhee, S.-K.; Karpfen, A. *Chem. Phys. Lett.* **1988**, *120*, 199. (e) Oszczapowicz, J.; Jaroszewska-Manaj, J.; Golimowska, K. *J. Chem. Soc., Perkin Trans. 2* **2000**, 2343. (f) Hilfiker, M. A.; Mysak, E. R.; Samet, C.; Maynard, A. *J. Phys. Chem. A* **2001**, *105*, 9972.
- (3) (a) Trudeau, G.; Dumas, J.-M.; Dupuis, P.; Sandorfy, C. *Top. Curr. Chem.* **1980**, *93*, 91. (b) Budzinsky, M.; Fiedler, A. *Z. Synthesis* **1989**, 858. (c) Boldeskul, I. E.; Tsymbal, I. F.; Ryltsev, E. V.; Latajka, Z.; Barnes, A. *J. J. Mol. Struct.* **1997**, *436*, 167. (d) Hobza, P.; Spirko, V.; Selze, H. L.; Schlag, E. W. *J. Phys. Chem. A* **1998**, *102*, 2501. (e) Hobza, P.; Havlas, Z. *Chem. Phys. Lett.* **1999**, *303*, 447. (f) Karger, N.; Amorin da Costa, A. M.; Ribeiro-Claro, P. J. A. *J. Phys. Chem. A* **1999**, *103*, 8672. (g) Masella, M.; Flament, J. P. *J. Chem. Phys.* **1999**, *110*, 7245. (h) Mizumo, K.; Inafuji, S.; Ochi, T.; Ohta, T.; Maeda, S. *J. Phys. Chem. B* **2000**, *104*, 11001. (i) Gu, Y.; Karr, T.; Scheiner, S. *J. Am. Chem. Soc.* **1999**, *121*, 9411. (j) Gu, Y.; Karr, T.; Scheiner, S. *J. Mol. Struct.* **2000**, *500*, 441. (k) Choi, H. S.; Kim, K. S. *J. Phys. Chem. B* **2000**, *104*, 11006. (l) Vargas, R.; Garza, J.; Dixon, D. A.; Hay, B. P. *J. Am. Chem. Soc.* **2000**, *122*, 4750. (m) Kryachko, E. S.; Zeegers-Huyskens, Th. *J. Phys. Chem. A* **2001**, *105*, 7118. (n) Reimann, B.; Buchhold, K.; Vaupel, S.; Brutschy, B.; Havlas, Z.; Spirko, V.; Hobza, P. *J. Phys. Chem. A* **2001**, *105*, 5560. (p) Wang, Y.; Balbuena, P. B. *J. Phys. Chem. A* **2001**, *105*, 9972.
- (4) See for example (a) *The Hydrogen Bond. Recent Developments in Theory and Experiments*; Schuster, P.; Zundel, G.; Sandorfy, C., Eds.; North-Holland Publishing Company: Amsterdam, 1976. (b) Ratajczak, H.; Orville-Thomas, W. J. *Molecular Interactions*; John Wiley & Sons: Chichester, 1980.
- (5) (a) Dougherty, R. C.; Dalton, J.; Roberts, J. D. *Org. Mass Spectrom.* **1974**, *8*, 77. (b) Sullivan, S. A.; Beauchamp, J. L. *J. Am. Chem. Soc.* **1976**, *98*, 1160. (c) French, M. A.; Ikuta, S.; Kebarle, P. *Can. J. Chem.* **1982**, *60*, 1907. (d) Larson, J. W.; McMahon, T. B. *J. Am. Chem. Soc.* **1983**, *105*, 2944. (e) Larson, J. W.; McMahon, T. B. *J. Am. Chem. Soc.* **1984**, *106*, 517. (f) Hiraoka, K.; Katsuragawa, J.; Sugiyama, T.; Kojima, S. *J. Am. Chem. Soc. Mass Spectrom.* **2001**, *12*, 144. (g) Chabynyc, M. L.; Brauman, J. I. *J. Am. Chem. Soc.* **1998**, *120*, 10863. Chabynyc, M. L.; Brauman, J. I. *J. Am. Chem. Soc.* **2000**, *122*, 8739.
- (6) (a) Novoa, J. J.; Whanbo, M.-H. *Chem. Phys. Lett.* **1991**, *180*, 241. (b) Hobza, P.; Havlas, Z. *Chem. Rev.* **2000**, *1000*, 4253.
- (7) (a) Wild, D. A.; Loh, Z. M.; Wolyneec, P. P.; Weiser, E. J.; Buske, E. *J. Chem. Phys. Lett.* **2000**, *332*, 531. (b) Hiraoka, K.; Mizuno, T.; Iino, T.; Eguchi, D.; Yamabe, S. *J. Phys. Chem. A* **2001**, *105*, 4887.
- (8) (a) Ensing, B.; Meijer, E. J.; Blochl, P. E.; Baerends, E. J. *J. Phys. Chem. A* **2001**, *105*, 3300. (b) Hauschildt, J.; Schinke, R.; Schmatz, S.; Botschwina, P. *Phys. Chem. Chem. Phys.* **2001**, *3*, 2275. (c) Schmatz, S.; Botschwina, P.; Hauschildt, J.; Schinke, R. *J. Chem. Phys.* **2001**, *114*, 5233. (d) Ohmiya, K.; Kato, S. *Chem. Phys. Lett.* **2001**, *348*, 75. (e) Parthiban, S.; de Oliveira, G.; Martin, J. M. L. *J. Phys. Chem. A* **2001**, *105*, 895.
- (9) Boys, S. F.; Bernardi, F. *Mol. Phys.* **1979**, *19*, 663.
- (10) Reed, A. E.; Curtiss, L. A.; Weinhold, F. *Chem. Rev.* **1988**, *88*, 899.
- (11) Frisch, M. J.; Trucks, G. W.; Schlegel, H. B.; Scuseria, G. E.; Robb, M. A.; Cheeseman, J. R.; Zakrzewski, V. G.; Montgomery, J. A., Jr.; Stratmann, R. E.; Burant, J. C.; Dapprich, S.; Millam, J. M.; Daniels, A. D.; Kudin, K. N.; Strain, M. C.; Farkas, O.; Tomasi, J.; Barone, V.; Cossi, M.; Cammi, R.; Mennucci, B.; Pomelli, C.; Adamo, C.; Clifford, S.; Ochterski, J.; Petersson, G. A.; Ayala, P. Y.; Cui, Q.; Morokuma, K.; Malick, D. K.; Rabuck, A. D.; Raghavachari, K.; Foresman, J. B.; Cioslowski, J.; Ortiz, J. V.; Stefanov, B. B.; Liu, G.; Liashenko, A.; Piskorz, P.; Komaromi, I.; Gomperts, R.; Martin, R. L.; Fox, D. J.; Keith, T.; Al-Laham, M. A.; Peng, C. Y.; Nanayakkara, A.; Gonzalez, C.; Challacombe, M.; Gill, P. M. W.; Johnson, B. G.; Chen, W.; Wong, M. W.; Andres, J. L.; Head-Gordon, M.; Replogle, E. S.; Pople, J. A. *Gaussian 98*, revision A.5; Gaussian, Inc.: Pittsburgh, PA, 1998.
- (12) Kawahara, S. I.; Uchimaru, T.; Taira, K. *Chem. Phys.* **2001**, *273*, 207 and references therein.
- (13) Kryachko, E. S.; Zeegers-Huyskens, Th. *J. Mol. Struct.* In press.
- (14) Lias, S. G.; Bartmess, J. E.; Liebman, J. F.; Holmes, J. L.; Levin, R. D.; Mallard, W. G. *J. Phys. Chem. Ref. Data, Suppl.*, **1988**, *17*. Experimental values (kcal mol⁻¹) of the DPE: CH₄, 418; CH₃F, 409; CH₂F₂, 389; CHF₃, 376; CH₂Cl, 396; CH₂Cl₂, 374; CHCl₃, 358. Experimental values (kcal mol⁻¹) of the PA of the X⁻ anions: F⁻, 372; Cl⁻, 333; OH⁻, 390.
- (15) All geometric and vibrational data are available from the authors.
- (16) Badger, G. M.; Bauer, S. H. *J. Chem. Phys.* **1937**, *5*, 839.
- (17) Rozenberg, M.; Loewenschuss, A.; Marcus, Y. *Phys. Chem. Chem. Phys.* **2000**, *2*, 2699.
- (18) (a) Sandorfy, C. *Top. Curr. Chem.* **1984**, *120*, 42. (b) Rospenk, M.; Zeegers-Huyskens, Th. *J. Phys. Chem.* **1997**, *101*, 8428. (c) Leroux, N.; Samyn, C.; Zeegers-Huyskens, Th. *J. Mol. Struct.* **1998**, *448*, 209. (d) Pawelka, Z.; Zeegers-Huyskens, Th. *Vib. Spectrosc.* **1998**, *18*, 41. (e) Luck, W. A. P.; Wess, T. *Can. J. Chem.* **1991**, *69*, 1819. (f) Ojamae, L.; Shavitt, L.; Singer, S. H. *Int. J. Quantum Chem., Quantum Chem. Symp.* **1995**, *29*, 567.
- (19) (a) Hartmann, M.; Wetmore, S. D.; Radom, L. *J. Phys. Chem. A* **2001**, *105*, 4470. (b) Hartmann, M.; Wetmore, S. D.; Radom, L. *J. Phys. Chem. A* **2001**, *105*, 8718. (c) Scheiner, S.; Grabowski, S. J.; Kar, T. *J. Phys. Chem. A* **2001**, *105*, 10607.
- (20) (a) Chandra, A. K.; Nguyen, M. T.; Uchimaru, T.; Zeegers-Huyskens, Th. *J. Phys. Chem. A* **1999**, *103*, 8853. (b) Kryachko, E. S.; Nguyen, M. T.; Zeegers-Huyskens, Th. *J. Phys. Chem. A* **2001**, *105*, 1934.
- (21) Schaftenaar, G.; Noordik, J. H. *J. Comput.-Aided Mol. Design*, **2000**, *14*, 123.
- (22) (a) Huyskens, P. L. *J. Am. Chem. Soc.* **1977**, *99*, 2578. (b) Rulinda, J. B.; Zeegers-Huyskens, Th. *Bull. Soc. Chim. Belg.* **1976**, *84*, 159.
- (23) (a) Hobza, P. *Phys. Chem. Chem. Phys.* **2001**, *3*, 2555. (b) van der Veken, B. J.; Herrebout, W. A.; Szostak, R.; Shchepkin, D. N.; Havlas, Z.; Hobza, P. *J. Am. Chem. Soc.* **2001**, *123*, 12290.